that group of carriers which makes the greatest contribution to the nonlocal conductivity. There is a group of electrons in tungsten with an extremal shift (the section I [7]); however, for these electrons, the quantity $\partial S/\partial p_z$ differs by 30% from the corresponding value for the holes of the section A (at the limiting points of the electron Fermi surface, this difference is even greater). Therefore, the oscillations in the "–" polarization cannot be connected with the excitation of the electron doppleron.

[1]J. C. McGroddy, J. L. Stanford and E. A. Stern, Phys. Rev. **141**, 437 (1966).
[2]L. M. Fisher, V. V. Lavrova, V. A. Yudin, O. V. Konstantinov and V. G. Skobov, Zh. Eksp. Teor. Fiz. **60**, 759 (1971) [Sov. Phys. JETP **33**, 410 (1971)].
[3]V. F. Gantmakher and É. A. Kaner, Zh. Eksp. Teor. Fiz. **48**, 1572 (1965) [Sov. Phys. JETP **21**, 1053 (1965)].
[4]V. V. Lavrova, S. V. Medvedev, V. G. Skobov, L. M. H. Fisher and V. A. Uydin, Zh. Eksp. Teor. Fiz. **64**, 1839 (1973) [Sov. Phys. JETP **37**, 929 (1973)].
[5]I. M. Vitebskiĭ, V. T. Vitchinkin, A. A. Galkin, Yu. S. Ostroukhov, O. A. Panchenko, D. T. Tsymbal and A. N. Cherkasov, Fiz. Nizkikh Temp. 1, 400 (1975) [Sov. J. Low Temp. Phys. **1**, 200 (1975)].
[6]R. F. Girvan, A. V. Gold, R. A. Phillips, J. Phys. Chem. Sol. **29**, 1485 (1968).
[7]D. E. Soule, and J. C. Abele, Phys. Rev. Lett. **23**, 1287 (1969).
[8]V. V. Boĭko and V. A. Gasparov, Zh. Eksp. Teor. Fiz. **61**, 2362 (1971) [Sov. Phys. JETP, **34**, 1266 (1972)].
[9]V. G. Skobov, L. M. Fisher, A. S. Chernov and V. A. Yudin, Zh. Eksp. Teor. Fiz. **67**, 1218 (1974) [Sov. Phys. JETP **40**, 605 (1975)].
[10]É. A. Kaner and V. G. Skobov, Adv. in Phys. **17**, 605 (1968).
[11]Yu. S. Ostroukhov, O. A. Panchenko and A. A. Kharlamov, Zh. Eksp. Teor. Fiz. **70**, 1838 (1976) [Sov. Phys. JETP **43**, 957 (1976)].
[12]I. F. Voloshin, S. V. Medvedev, V. G., Skobov, L. M. Fisher and A. S. Chernov, Pis'ma Zh. Eksp. Teor. Fiz. **23**, 553 (1976) [JETP Lett. **23**, 507 (1976)].
[13]I. F. Voloshin, S. V. Medvedev, V. G. Skobov, L. M. Fisher and A. S. Chernov, Zh. Eksp. Teor. Fiz. **71**, 1555 (1976) [Sov. Phys. JETP **44**, 814 (1976)].
[14]D. S. Falk, Phys. Rev. B **3**, 1973 (1971).

Translated by R. T. Beyer

Penetration of a magnetic field into a Josephson junction

G. F. Zharkov and S. A. Vasenko

P. N. Lebedev Institute of Physics, USSR Academy of Sciences

(Submitted 18 July 1977)
Zh. Eksp. Teor. Fiz. **74**, 665–680 (February 1978)

All the possible types of solutions to the nonlinear equation for the distribution of a static magnetic field in a Josephon barrier of finite width are described. For each type of solution corresponding to the boundary-value problem, the Cauchy problem, which allows a unique association of a definite set of "initial" data with each solution, is formulated and solved by numerical methods. The magnetization curves of the Josephson junction are found for several barrier-width values ($L = 1, 4, 10$). The question of the stability of the static solutions, including those that are anomalous in comparison with the usual Meissner-type solutions, is investigated. Examples of the numerical solution of the nonstationary, nonlinear equation that illustrate the dynamics of the establishment of the static solutions are given.

PACS numbers: 74.30.Ci, 74.50.+r

The question of the penetration of a static magnetic field into a Josephson junction has been repeatedly discussed in the literature.[1-7] The one-dimensional linear vortex structure that arises in the barrier in the case of an infinitely wide barrier has been analytically described by Kulik,[2,3] while for the case of a barrier of finite width some examples of the field distribution in the junction have been obtained with the aid of numerical methods by Owen and Skalapino.[4] A number of distinctive features of the penetration of a magnetic field into a junction of finite width have been noted in a paper by one of the present authors[7] (in particular, the unevenness of the entry of the individual vortices into the junction, as well as the presence of "superheating" and "supercooling" fields that limit the existence domain of a given number of vortices in a weak superconductor).

The present paper is devoted to a more detailed—in comparison with Refs. 4 and 7—study of the character of the penetration of a magnetic field into a Josephson barrier of finite width. The boundary-value problem for the nonlinear equation governing the steady-state magnetic-field and current distributions inside the barrier turns out to be nonunique: for specified values of the field at the junction edges the equation has several solutions describing different field distributions inside the barrier. In the present paper the boundary-value problem is reduced to an equivalent Cauchy problem; this procedure allows us to uniquely associate a definite set of "initial" data with each solution and find all the solutions of the problem. Below we describe all the possible types of solutions (Sec. 1) and find the integral relations that allow the determination of the initial data (i.e., the values of the function and its derivative at one of the barrier edges) in terms of the parameters of the boundary-value problem (Sec. 2). Dependences found with the aid of a computer (and, in a number of cases, analytically) are illustrated with graphs. Besides the usual Meissner-type solutions,[1-7] in which the field falls off into the barrier in comparison with its value at the edges, we describe anamalous solutions in which the field increases into the barrier, or else there obtains an asymmetric distribution of the field, as well as solutions corresponding to more complex field configurations, in particular, to an array of vortices with alternating signs.

We find the free-energy functions of the Josephson barrier in an external field for the various types of solutions (Sec. 3), and present graphs illustrating the shape

0038-5646/78/4702-0350$02.40

of the magnetization curves of barriers of different widths (Sec. 4).

In Sec. 5 we investigate the question of the stability of the obtained solutions. We show that the anomalous solutions are unstable, but that they can be realized in the course of a transition of the system from one stable state into another. The numerical solution of the nonstationary, nonlinear equation allows us to trace the nature of the formation of the static solutions. Under certain conditions the field and current distributions in the barrier can, for a long time, correspond to an unstable state; therefore, such states can, in principle, manifest themselves in experiment.

1. The basic equation describing the distribution of a static magnetic field in a Josephson junction has the form[1-7]

$$\frac{d^2\varphi}{dx^2}=\sin\varphi, \tag{1}$$

where the quantity $\varphi(x)$ (the so-called phase difference of the wave functions of the superconductors) is related to the magnetic field in the barrier:

$$\frac{d\varphi}{dx}=H(x). \tag{2}$$

In (1) and (2) we have used dimensionless quantities: the coordinate is measured in units of λ_J ($\lambda_J\sim 0.1$ mm is the characteristic penetration distance of the field into the weak superconductor), while the magnetic field is measured in units of $H_J=\Phi_0/2\pi\lambda_J\Lambda$ (Φ_0 is the flux quantum, $\Lambda\sim 10^{-5}$ cm is the penetration depth of the field into a bulk superconductor; usually, $H_J\sim 0.1-1$ G). The boundary conditions for the problem of the penetration of an external field, H_e, into a barrier of width L have the form

$$\left.\frac{d\varphi}{dx}\right|_{x=0}=\left.\frac{d\varphi}{dx}\right|_{x=L}=H_e. \tag{3}$$

The solutions to Eq. (2) that satisfy the conditions (3) are given in an implicit form in terms of elliptic integrals, and can be of two types.

The first type of solutions is given by the formulas

$$\begin{gathered}x=\frac{1}{2}\int_{\varphi(0)}^{\varphi(x)}\frac{dy}{R(y)},\quad R(y)=\left\{\sin^2\frac{y}{2}+\alpha^2\right\}^{1/2}\geqslant 0,\\ H(x)=2R(\varphi(x)),\quad \alpha^2=\frac{H_e^2}{4}-\sin^2\frac{\varphi(0)}{2}\geqslant 0,\\ \varphi(L)=\pm\varphi(0)+2\pi n,\end{gathered} \tag{4}$$

where n is an arbitrary whole number.

The second type of solutions is given by the formulas

$$\begin{gathered}x=\frac{1}{2}\int_{\varphi(0)}^{\varphi(x)}\frac{dy}{\xi(y)R(y)},\quad R(y)=\left\{\sin^2\frac{y}{2}-\beta^2\right\}^{1/2}\geqslant 0,\\ H(x)=2\xi(x)R(\varphi(x)),\quad \beta^2=\sin^2\frac{\varphi(0)}{2}-\frac{H_e^2}{4}\geqslant 0,\quad \xi(x)=\operatorname{sign}H(x)=\pm 1,\end{gathered} \tag{5}$$

with $\varphi(L)=\varphi(0)$ or $\varphi(L)=2\pi-\varphi(0)$. These solutions can be expressed[2-6] in terms of the Jacobi elliptic functions, but we prefer to deal directly with the integral representations (4) and (5).

To elucidate the difference in character of the solutions (4) and (5), let us note that Eq. (1) is formally analogous to the equation for a compound pendulum without friction. It is known that the solutions of this equation can be of two types.[8] In one case the solutions correspond to the rotation of the pendulum about an axis, the angle, φ, of rotation increasing without restriction: by 2π after each complete rotation (it will become clear from what follows that solutions of the type (4) are analogous to the rotary motion of the pendulum). In the other case the solutions correspond to oscillations of the pendulum about an equilibrium position without rotation about an axis, the angle φ varying in this case within the limits $0\leqslant\varphi\leqslant 2\pi$ (it will become clear from what follows that solutions of the type (5) are analogous to the oscillatory motion of the pendulum). The sign function $\xi(x)=\pm 1$ in (5) then takes into account the change in the direction of the "velocity" of the motion. The foregoing is illustrated by Figs. 1a and 1b, which depict the characteristic behavior of the solutions of Eq. (1) for the two indicated cases, the heavy points on the curves indicating the values of certain solutions that satisfy the boundary conditions (3), i.e., the values of the derivative $d\varphi/dx|_{x=0}$. Notice that if $\varphi(x)$ is a solution to the problem, then $\varphi(x)+2\pi m$ is also a solution.

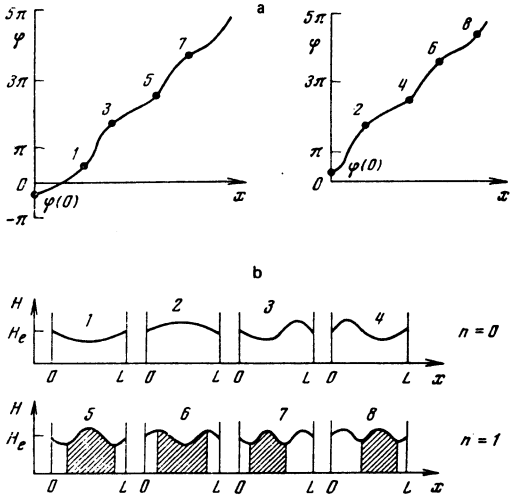

FIG. 1. a) Schematic representation of the dependence $\varphi(x)$ corresponding to a solution of the type (4) (analogous to the rotary motion of a pendulum). The two samples of the curves correspond to the two possible ranges of variation of $\varphi(0)$ noted in the text, namely, $-\pi<\varphi(0)<0$ and $0<\varphi(0)<\pi$. The heavy points on the curves correspond to the values at which $\varphi'(L)=\varphi'(0)$. These points are given numbers indicating the number of the corresponding solution (see text). For example, the solution 4 starts from the point $\varphi(0)$ for $x=0$ and ends at the point 4 shown on the curve. b) Distribution of the field $H=d\varphi/dx$ in the barrier for different solutions (schematic). The solutions 1 and 3 are the basic ones in the series of solutions with odd numbers. The solutions 5, 7, etc., are formed by the addition of one or a larger number of vortices (n denotes the integral number of vortices in the given distribution). Similarly, the solutions 2 and 4 generate a series of solutions with even numbers. The hatched regions correspond to one vortex.

Therefore, it is sufficient to limit ourselves to the study of the solutions for which the $\varphi(0)$ values lie in the interval $-\pi \leqslant \varphi(0) \leqslant \pi$ (see Figs. 1a and 2a).

We shall number the solutions of the type (4) (Fig. 1) in the following manner. If the boundary value $\varphi(0) < 0$, then we shall characterize the solutions by odd numbers, $N = 1, 3, 5, \ldots$, etc., setting in correspondence with these numbers the following possible values of $\varphi(L)$:

N	1	3	5	7	9
$\varphi_N(L)$:	$\lvert\varphi(0)\rvert$	$2\pi - \lvert\varphi(0)\rvert$	$2\pi + \lvert\varphi(0)\rvert$	$4\pi - \lvert\varphi(0)\rvert$	$4\pi + \lvert\varphi(0)\rvert$

etc., or

$$\varphi_{4n+1}(L) = 2\pi n + |\varphi(0)|, \quad \varphi_{4n+3}(L) = 2\pi(n+1) - |\varphi(0)|, \quad \varphi(0) < 0, \; n = 0, 1, 2, \ldots \tag{6}$$

The basic solutions in this series are the solutions 1 and 3; the others are obtained from them by the addition of an integral number of cycles (see Fig. 1), corresponding to the presence in the junction of a certain whole number of vortices. The addition of an extraneous cycle (vortex) corresponds to a transition in the formulas (6) from the solution characterized by the number n to the solution $n+1$.

If the boundary value $\varphi(0) > 0$, then we shall number the solutions by even numbers, 2, 4, 6, etc., setting in correspondence with these numbers the following possible values:

N	2	4	6	8
$\varphi_N(L)$:	$2\pi - \varphi(0)$	$2\pi + \varphi(0)$	$4\pi - \varphi(0)$	$4\pi + \varphi(0)$

etc., or

$$\varphi_{4n+2}(L) = 2\pi(n+1) - \varphi(0), \quad \varphi_{4n+4}(L) = 2\pi(n+1) + \varphi(0), \quad \varphi(0) > 0, \; n = 0, 1, 2, \ldots \tag{7}$$

The basic solutions in this series are the solutions 2 and 4; the others are obtained from them through the addition of an integral number, n, of cycles (see Fig. 1), which corresponds to a transition to a solution with n additional vortices.

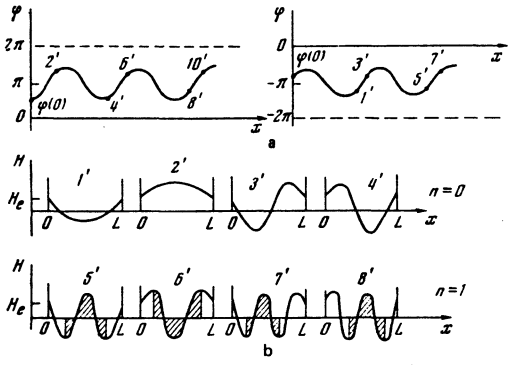

FIG. 2. a) Behavior of a solution, $\varphi(x)$, of the type (5) (analogous to the oscillatory motion of a pendulum). b) Schematic distribution of the field $H = d\varphi/dx$ in the barrier. The basic solutions are those numbered $1' - 4'$; all the other solutions are obtained from these basic solutions by the addition of integral numbers of vortices. The solutions $5' - 8'$ are respectively obtained from $1' - 4'$ by the addition of one vortex.

The solutions of the type (5) are numbered in analogous fashion (see Fig. 2): we shall characterize these functions by primed numerical subscripts (1′, 2′, etc.) and set them in correspondence with the following values of $\varphi_{N'}(L)$:

$$\varphi_{(4n+1)'}(L) = -2\pi + |\varphi(0)|, \quad \varphi_{(4n+3)'}(L) = -|\varphi(0)|, \quad \varphi(0) < 0; \tag{6'}$$

$$\varphi_{(4n+2)'}(L) = 2\pi - \varphi(0), \quad \varphi_{(4n+4)'}(L) = \varphi(0), \quad \varphi(0) > 0. \tag{7'}$$

The basic solutions here are the solutions 1′, 3′ (for $\varphi(0) < 0$) and 2′, 4′ (for $\varphi(0) > 0$); the rest are obtained from them by the addition of an integral number of cycles (Fig. 2). Notice that these solutions describe states with oppositely directed vortices (i.e., the magnetic fields in neighboring vortices have opposite directions: see Fig. 2b).

The above-enumerated solutions exhaust all the possible types of solutions of the static problem formulated in (1)–(3).[1)]

2. It is not difficult to obtain integral relations characterizing each of the possible solutions. Indeed, substituting the value $x = L$ into (4), we find

$$L = \frac{1}{2}\int_{\varphi(0)}^{\varphi_N(L)} \frac{dx}{R(x)} = F_N(\varphi(0)), \tag{8}$$

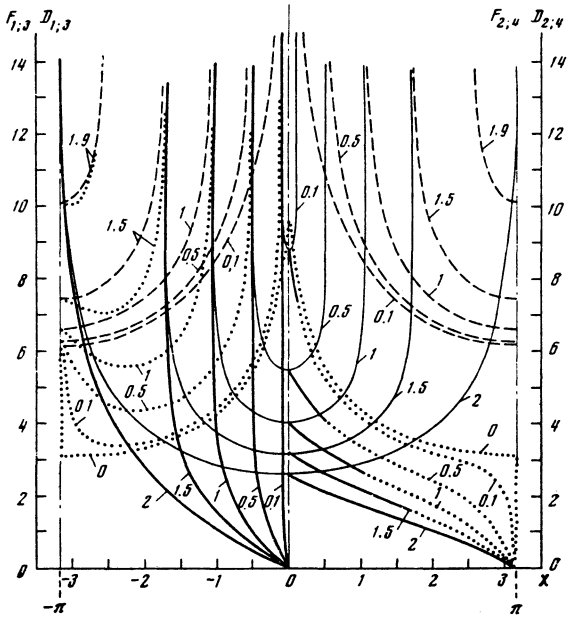

FIG. 3. Plots of the functions $F_N(\chi)$ and $D_{N'}(\chi)$. The heavy curves depict the functions $F_1(\chi)$ (for $\chi < 0$) and the functions $F_2(\chi)$ for $\chi > 0$). The thin continuous lines represent the functions $F_3(\chi)$ ($\chi < 0$) and $F_4(\chi)$ ($\chi > 0$). The dotted lines give the functions $D_1(\chi)$ ($\chi < 0$) and $D_2(\chi)$ ($\chi > 0$). The broken lines give the functions $D_3(\chi)$ ($\chi < 0$) and $D_4(\chi)$ ($\chi > 0$). The numbers on the curves indicate the values of the parameter $H_2 \leqslant 2$. Drawing the horizontal straight lines $y = L$, and determining the points of their intersection with the curves shown, we find for the given L the possible roots of Eqs. (8), (9). It can be seen from the figure that, for example, the equation $L = D_1(\chi)$ has no roots for $L < \pi$, while the equations $L = D_{3,4}(\chi)$ have no roots for $L < 2\pi$. For a given value of L there exists a definite range of H_e values at which the solutuion with the number N is possible.

where the $\varphi_N(L)$ are defined in (6) and (7). The relations (8) are used for the determination of the boundary value $\varphi(0)$ as a function of H_e, L, and N. Introducing in place of $\varphi(0)$ the variable $\chi = |\varphi(0)|$, and carrying out simple transformations, we obtain for the right-hand side of (8) the expressions

$$F_1(-\chi)=\int_0^{\chi}\frac{dx}{R(x)},\quad F_2(\chi)=\int_0^{\pi-\chi}\frac{dx}{R(x)},$$

$$F_3(-\chi)=F_4(\chi)=\int_0^{\pi}\frac{dx}{R(x)}=V(\chi),\tag{9}$$

$$F_{4n+1}(-\chi)=F_1(-\chi)+nV(\chi),\ F_{4n+2}(\chi)=F_2(\chi)+nV(\chi),$$
$$F_{4n+3}(-\chi)=F_{4n+4}(\chi)=(n+1)V(\chi),$$
$$R(x)=\left\{\sin^2\frac{x}{2}+\frac{H_e^2}{4}-\sin^2\frac{\chi}{2}\right\}^{1/2},\quad 0\leqslant\chi\leqslant\chi_c,\quad \chi_c=2\arcsin\frac{H_e}{2}.$$

The functions $F_N(\pm\chi)$ for $N=1,2,3,4$ are depicted[2)] in Fig. 3 for values of $H_e\leqslant 2$ and in Fig. 4 for $H_e>2$. The points, χ_N, of $y=L$ coincide with the roots of Eq. (8), and allow us to determine the values of $\varphi_N(0)=\pm\chi_N$.

Similarly, we can derive the equations determining the values of $\varphi_{N'}(0)$ for the solutions of the type (5):

$$L=\frac{1}{2}\int_{\varphi(0)}^{\varphi_{N'}(L)}\frac{dx}{\xi(x)R(x)}=D_{N'}(\varphi(0)),\quad N'=1',2',\ldots,\tag{10}$$

where the functions $D_{N'}$ have the form

$$D_1(-\chi)=2\int_0^{\pi-A}\frac{dx}{r(x)}-2\int_{(\pi-A)/2}^{(2\pi-\chi-A)/2}\frac{dx}{r(x)},$$

$$D_2(\chi)=2\int_{(\chi-A)/2}^{(\pi-A)/2}\frac{dx}{r(x)},\quad D_3(-\chi)=D_4(\chi)=2\int_0^{\pi-A}\frac{dx}{r(x)}=W(\chi),\tag{11}$$

$$D_{4n+1}(-\chi)=D_1(-\chi)+nW(\chi),\ D_{4n+2}(\chi)=D_2(\chi)+nW(\chi),$$
$$D_{4n+3}(-\chi)=D_{4n+4}(\chi)=(n+1)W(\chi),$$
$$r(x)=(\sin(A+x)\sin x)^{1/2},\quad A=2\arcsin\left(\sin^2\frac{\chi}{2}-\frac{H_e^2}{4}\right)^{1/2},$$
$$\chi_c<\chi\leqslant\pi,\ 0\leqslant A\leqslant\pi.$$

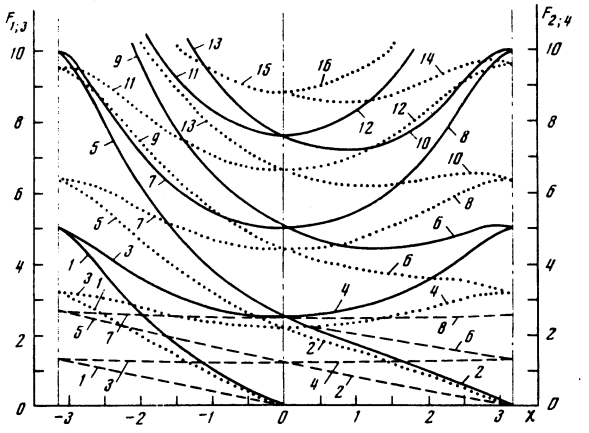

FIG. 4. Plots of the functions $F_N(\chi)$ for $H_e>2$. The numbers on the curves indicate the number of the solution. The heavy lines give the curves for $H_e=2.1$, the dotted for $H_e=2.5$, the dashed for $H_e=5$ (only part of the dashed lines are shown). The solution with the given number N in the field H_e corresponds to the point of intersection of the horizontal straight line $y=L$ with the curve F_N.

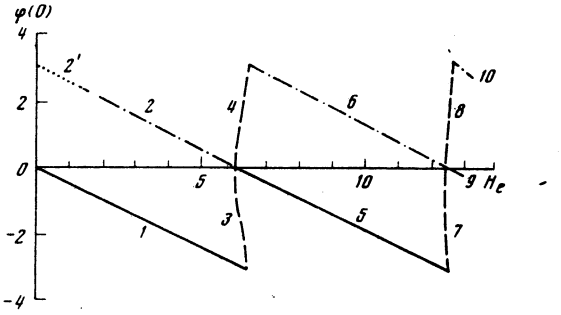

FIG. 5. The external-field (H_e) dependence of $\varphi(0)$ for $L=1$ in the Cauchy problem (12), which is equivalent to the original boundary-value problem (1)–(3). The numbers on the curves correspond to the mode of numeration of the solutions in the present paper. The numbers of the branches corresponding to the stable solutions are 1, 5, 9, etc. (the solid lines). The branches with the numbers 6, 10, etc. correspond to unstable solutions. The branches 4, 8, etc. correspond to nonsymmetric solutions. Their mirror image in the plane $x=L/2$ gives the nonsymmetric solutions determined by the branches 3, 7, etc.

The functions $D_{N'}$ for $N'=1'$, $2'$, $3'$, $4'$ are depicted in Fig. 3. There are no solutions of the type (5) for $H_e>2$ (for the parameter β^2 in (5) cannot be negative). The points, $\chi_{N'}$, of intersection of the curves $D_{N'}(\pm\chi)$ with the straight lines $y=L$ give the roots of Eq. (10): $\varphi_{N'}(0)=\pm\chi_{N'}$.

Figures 5–7 show the $\varphi_N(0)$- and $\varphi_{N'}(0)$-versus-H_e curves for $L=1,4$, and 10.

Having determined the $\varphi(0)$ values from (8) and (10) (see Figs. 3–7), we can formulate the Cauchy problem for Eq. (1):

$$\varphi|_{x=0}=\varphi(0),\quad \left.\frac{d\varphi}{dx}\right|_{x=0}=H_e.\tag{12}$$

For the found value of $\varphi(0)$, the solution satisfying (12) will automatically satisfy the condition $d\varphi/dx|_{x=L}=H_e$ as well. The reduction of the boundary-value problem (3) to the Cauchy problem (12) turns out to be convenient for the purpose of carrying out numerical computations, as well as for the general classification of the solutions. Examples, obtained by solving the Cauchy problem (12), of the field and current distributions in barriers of different widths are given in Sec. 4.

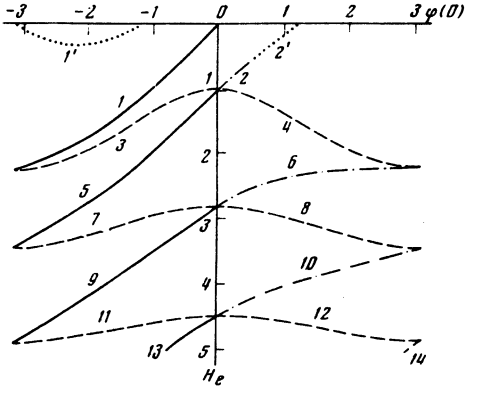

FIG. 6. Same as in Fig. 5, but for $L=4$.

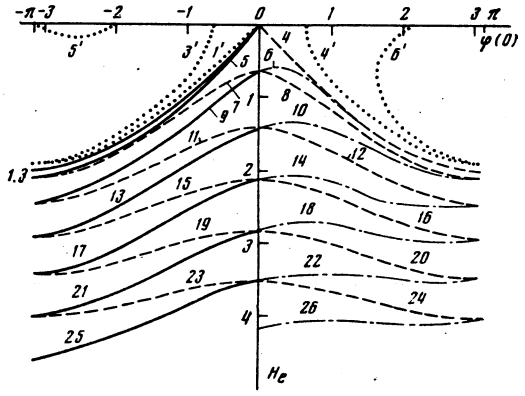

FIG. 7. Same as in Fig. 5, but for $L = 10$.

3. The above-obtained dependences of the parameter $\varphi(0)$ on H_e allow us to determine easily the value of the *mean field*, $\overline{H}_N$, in the barrier, i.e., to find the magnetization curves of the weak superconductor. In fact, we have

$$\overline{H}_N = \frac{1}{L}\int_0^L H(x)\,dx = \frac{\varphi_N(L) - \varphi_N(0)}{L}, \tag{13}$$

from which we obtain the following expressions for type-(4) solutions with different numbers N (see (6), (7)):

$$\begin{aligned} \overline{H}_{4n+1} &= \{2\pi n + 2|\omega_{4n+1}(0)|\}/L, \\ \overline{H}_{4n+2} &= \{2\pi(n+1) - 2\varphi_{4n+2}(0)\}/L, \\ \overline{H}_{4n+3} &= \overline{H}_{4n+4} = 2\pi(n+1)/L, \quad n = 0, 1, 2, \ldots \end{aligned} \tag{14}$$

Similarly, we find for type-(5) solutions with different numbers N' (see (6'), (7')):

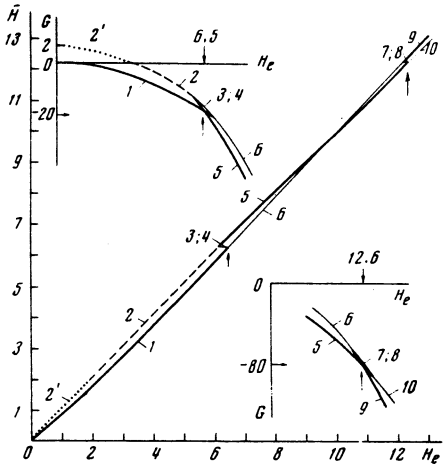

FIG. 8. Dependence of the mean field in the barrier on the external field (magnetization curves) for $L = 1$. The numbers on the curves indicate the numbers of the corresponding solutions. The inserts show the free energy, computed from the formulas (16)–(19). The curves represented by the heavy lines correspond to stable solutions. The arrows indicate the field values, H_{eq}, at which the system should, under conditions of thermodynamic equilibrium, go over from one branch to another with a unit change in the number of vertices. The sections of the heavy curves lying in the regions $H \lesssim H_{eq}$ correspond to possible metastable states (superheating and supercooling).

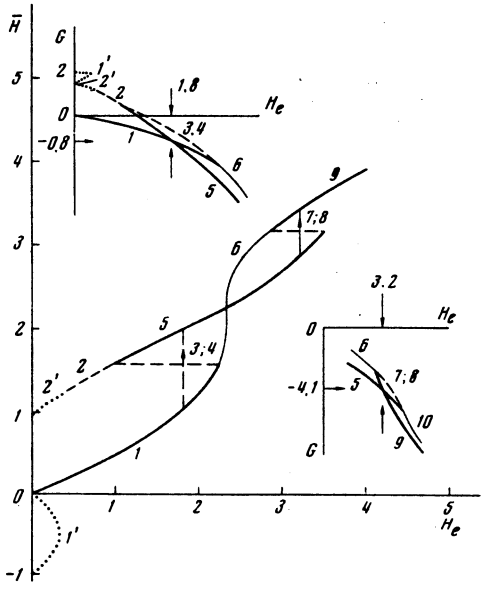

FIG. 9. Same as in Fig. 8, but for $L = 4$.

$$\begin{aligned} \overline{H}_{(4n+1)'} &= \{-2\pi + 2|\varphi_{(4n+1)'}(0)|\}/L, \\ \overline{H}_{(4n+2)'} &= \{2\pi - 2\varphi_{(4n+2)'}(0)\}/L, \\ \overline{H}_{(4n+3)'} &= \overline{H}_{(4n+4)'} = 0, \quad n = 0, 1, 2, \ldots \end{aligned} \tag{15}$$

Figures 8–10 show the $\overline{H}_N$ and $\overline{H}_{N'}$ versus H_e curves for $L = 1, 4$, and 10.

To each point on the curves in Figs. 8–10 corresponds its own field and current configuration inside the barrier. (Examples of the possible static distributions of the field are indicated in Figs. 1 and 2 and in Sec. 4.) When the external field is changed, the field configuration in the barrier and, consequently, the energy of this state change. The question arises of the comparison of the energies of the various states that are possible in a given field H_e. It is clear that it is advantageous for the system to be in the state that possesses the lowest free energy. This question is discussed in Sec. 4.

4. To find the external-field values at which a thermodynamic-equilibrium transition from a solution of number N to a solution with a different number can occur, it is necessary to compare the Gibbs free energies for states with different N.

Let us write down the Gibbs potential[3, 6, 7] for the state of number N (similarly for N'):

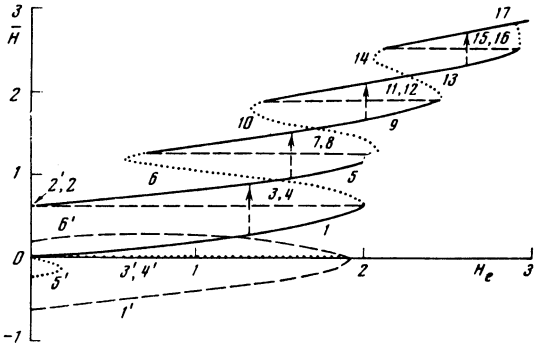

FIG. 10. Same as in Fig. 8, but for $L = 10$.

$$G_N(L, H_e) = \mathcal{E}_N(L, H_e) - \bar{H}_N H_e, \tag{16}$$

where $\mathcal{E}_N$ corresponds to the internal energy of the barrier, while the term $\bar{H}_N H_e$ corresponds to the change in the sample energy in the external field. Taking for $\mathcal{E}_N$ the expression[3, 6, 7]

$$\mathcal{E}_N = \frac{1}{L}\int_0^L \left\{1-\cos\varphi_N(x) + \frac{1}{2}\left(\frac{d\varphi_N}{dx}\right)^2\right\} dx, \tag{17}$$

going over from the variable x to the variable φ, and carrying out simple transformations, we obtain for the various N in the case of type-(4) solutions the expressions

$$\begin{aligned}
\mathcal{E}_{4n+1} &= -2\alpha^2 + \frac{8}{L}T_1 + \frac{8}{L}nT_2,\\
\mathcal{E}_{4n+2} &= -2\alpha^2 - \frac{8}{L}T_1 + \frac{8}{L}(n+1)T_2,\\
\mathcal{E}_{4n+3} &= \mathcal{E}_{4n+4} = -2\alpha^2 + \frac{8}{L}(n+1)T_2,
\end{aligned} \tag{18}$$

where $n = 0, 1, 2, \ldots$, $\alpha^2 = \frac{1}{4}H_e^2 - \sin^2(\varphi_N(0)/2)$.

$$T_1 = \int_0^{|\varphi_N(0)|/2} (\alpha^2+\sin^2\varphi)^{-1/2}\, d\varphi, \qquad T_2 = \int_0^{\pi/2} (\alpha^2+\sin^2\varphi)^{-1/2}\, d\varphi.$$

In the case of solutions of the type (5), we find, according to (17) the expressions

$$\begin{aligned}
\mathcal{E}_{1'} &= 2\sin^2\frac{A}{2} + \frac{16}{L}T_1' - \frac{8}{L}T_2',\\
\mathcal{E}_{2'} &= 2\sin^2\frac{A}{2} + \frac{8}{L}T_2', \qquad \mathcal{E}_{3'} = \mathcal{E}_{4'} = 2\sin^2\frac{A}{2} + \frac{8}{L}T',\\
T_1' &= \int_0^{(\pi-A)/2} r(\varphi)\, d\varphi, \qquad T_2' = \int_{(|\varphi(0)|-A)/2}^{(\pi-A)/2} r(\varphi)\, d\varphi,\\
T' &= \int_0^{\pi-A} r(\varphi)\, d\varphi.
\end{aligned} \tag{19}$$

The curves $G_N(H_e)$ and $G_{N'}(H_e)$, obtained on a computer with use of the formulas (16)–(19), are shown in the inserts in Figs. 8 and 9 for $L = 1$ and 4. Under conditions of thermodynamic equilibrium, the system should trace the curve with the least free energy. An equilibrium transition of the system from one state into another is possible at the points of intersection of the G_N curves (in Figs. 8–10 the equilibrium field values, H_{eq}, corresponding to these points are indicated by arrows).

However, the transition from, for example, the state 1 into the state 5 (which has the lower energy when $H > H_{eq}$) should be accompanied by a reconstruction of the magnetic-field configuration in the barrier. Indeed, the states 1 have at the center of the barrier a field minimum, while the states 5 have a maximum (see Figs. 1b, 11, and 12). Therefore, these states are separated, so to speak, by a "kinetic barrier" (we mean that, to get the transition from 1 to 5 to occur, we must impart additional energy to the system to set the electrons into the motion connected with the reconstruction of the field and current). As a result, it may turn out that the system, if it is in the state 1, will on crossing the point $H = H_{eq}$ remain in this state, which has a higher energy

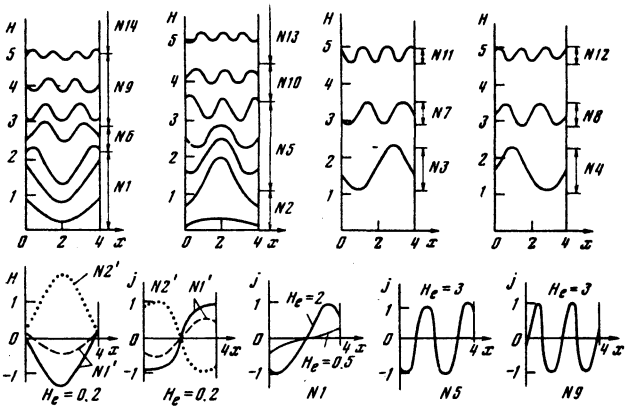

FIG. 11. Examples of static field and current distributions in a junction of length $L = 4$. The arrows indicate the existence domains of the solutions with the various numbers. The solutions 1, 5, and 9 are stable; the rest are unstable.

than the state 5, and once it has has got into the *state* 5, may remain in it when $H < H_{eq}$ (although the energy of the state 1 is smaller than the energy of the state 5 when $H < H_{eq}$). (Here we have an analog of the phenomena of superheating and supercooling for superconducting films in a magnetic field.[9]) It is clear that the boundaries of the regions of superheating, H_{sn}, and supercooling, H_{un}, coincide with the end points of the corresponding solution.[7] A transition to a solution with a different number necessarily occurs at $H > H_{sn}$ (or $H < H_{un}$). Since in a given field the system can trace different curves, depending on which state it is in, it is clear that hysteresis phenomena are possible here.

Notice that as the external field, H_e, is increased, the mean field in the barrier can, in the case of sufficiently small L, vary smoothly, tracing the sequence of curves 1, 6, 9 (see Figs. 8, 9 and 11, 12 for $L = 1$ and 4). When the field is subsequently decreased, the system can retrace in succession the curves 1, 6, 9, ..., i.e., there will be no hysteresis in this case. On the other

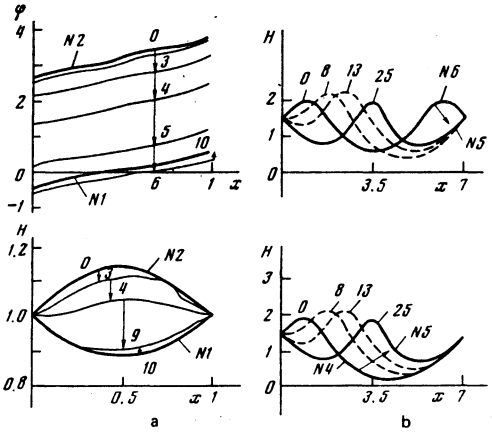

FIG. 12. Relaxation of unstable distributions (2, 4, 6) to stable ones (1, 5): a) $H_e = 1$, $L = 1$; b) $H_e = 1.5$, $L = 7$. The numbers on the curves indicate the moments of time in units of τ; the arrows indicate the direction of movement of the solutions. At the initial moment $t = 0$ the solution to Eq. (20) was given in the form of the static distribution 2, 4, or 6 and left to itself ($\varphi(x, t = 0) = 0$), the evolution of the unstable solution being determined by the presence of the increment (25).

hand, for a sufficiently wide barrier (e.g., for $L=10$: see Fig. 10), a transition from a solution to a solution cannot be smooth, and the field must penetrate the barrier in steps as the individual vortices enter it (cf. Ref. 7). Once the system gets into a new state, however, it can remain in that state as the field is decreased (right down to the end point, H_{un}, of the solution), i.e., there will be hysteresis. Under this circumstance, we could have discerned a connection with the known operating conditions of current-carrying Josephson junctions,[6,10] to wit, with the anhysteretic regime that obtains in the case of narrow barriers and the hysteretic regime in the case of wide barriers. In reality, the situation is more complicated.

It is clear that, for the system to be able to get, for example, into the state 6, which has a higher energy than the states 1 and 5 (see Figs. 8–10), the state 6 should be stable (metastable). The investigation, carried out in Sec. 5, of the stability of the obtained static solutions shows, however, that the solutions having the numbers 6, 10, etc. are unstable with respect to weak perturbations and, consequently, cannot be realized under static conditions. The stable solutions are the solutions 1, 5, 9,..., which are depicted in Figs. 8–10 by heavy lines. For this reason, the field in a narrow barrier cannot continuously trace the curves 1, 6, 9,... in succession, but should pass from one stable state (for example, 1) into another (for example, 5) discontinuously (over a sequence of nonstationary states; see Sec. 5). And having got into the state 5, the system may remain in this state as the external field is decreased, i.e., hysteretic behavior will occur. Thus, even narrow barriers located in an external field should behave in a hysteretic manner, and the field should penetrate them in steps. To be sure, the size of the hysteresis region in narrow barriers is small (cf. Figs. 8 and 10), and for $L\to 0$ (point barrier) the hysteresis region decreases to zero and a smooth (anhysteretic) penetration of the field into the barrier ensues. (For greater details apropos of the hysteresis phenomena experimentally observable in Josephson junctions, see, for example, Ref. 6).

5. As has already been noted, several different—in energy terms—states of the system are possible in a given external field. In order for the system to really have a change of getting into a state with a higher energy, it is necessary, in any case, that this state be stable (i.e., be a metastable state). The question of the stability of the states depicted in Figs. 8–11 should be resolved on the basis of a more general scheme that allows us to follow the development of the state in time under the influence of weak perturbations. For the description of the evolution of the system we can assume the equation[3,6]

$$\frac{\partial^2\varphi}{\partial t^2}+\beta\frac{\partial\varphi}{\partial t}-\frac{\partial^2\varphi}{\partial x^2}+\sin\varphi=0, \tag{20}$$

which goes over into Eq. (1) on neglecting the time derivatives. Here t is dimensionless time, expressed in units of $\tau=\lambda_J/c_0\sim 10^{-11}$ sec, where λ_J is the Josephson length, $c_0=c(L/\epsilon\Lambda)^{1/2}$ is the speed of electromagnetic waves in the junction, and ϵ is the permittivity of the barrier. The dissipative term $\beta\dot{\varphi}$ (the point denotes differentiation with respect to time) phenomenologically takes into account the ohmic losses in the barrier, which are connected with the appearance of a nonstationary electric field $E\sim\dot{\varphi}$ and a normal component of the current, $j_n=\sigma E$ (σ is the normal conductivity). This term guarantees the asymptotic extinction of the transient perturbations and the passage of the solution to the static regime described by Eq. (1).

The question of the stability of the solutions of the nonlinear partial differential equation, (20), is rather complicated, and its detailed analysis falls outside the framework of the present work. We restrict ourselves here to the presentation of preliminary results obtained in a numerical solution of Eq. (20) on a computer; these results allow us to get some indications of the nature of the stationary states of interest to us.

The investigation of the stability of the static solutions of Eq. (20) can be carried out, using the following standard procedure. Let $\varphi_0(x)$ be a static solution to Eq. (20) that coincides with a solution to Eq. (1). Writing the time-dependent solution in the form

$$\varphi(x,t)=\varphi_0(x)+\Psi(x,t),\quad |\Psi(x,t)|\ll 1 \tag{21}$$

and substituting (21) into (20), we find the linearized equation for the function $\Psi(x,t)$:

$$\frac{\partial^2\Psi}{\partial t^2}+\beta\frac{\partial\Psi}{\partial t}-\frac{\partial^2\Psi}{\partial x^2}+\cos\varphi_0\Psi=0. \tag{22}$$

Let us set $\Psi(x,t)=\psi(x)e^{\omega t}$ and go over to the Fourier components with respect to time. We then obtain for the amplitude $\psi(x)$ the equation

$$\frac{d^2\psi}{dx^2}+v(x)\psi=E\psi,\quad v(x)=-\cos\varphi_0(x),\quad E=\omega^2+\beta\omega. \tag{23}$$

We assume that the boundary conditions (3) are given and are independent; consequently, a solution to Eq. (23) should satisfy the following conditions:

$$\left.\frac{d\psi}{dx}\right|_{x=0}=\left.\frac{d\psi}{dx}\right|_{x=L}=0. \tag{24}$$

From Eq. (23) we can find under the conditions (24) the spectrum of the eigenvalues, E, at which the problem has a nontrivial solution. Knowing the eigenvalue E, we can easily determine the increments determining the evolution of the solution in time:

$$\omega_\pm=-{}^1/_2\beta\pm({}^1/_4\beta^2+E)^{1/2}. \tag{25}$$

It is clear from (25) that, for $E>0$, there necessarily exists an increasing solution of the form $\psi e^{\omega_+ t}$, $\omega_+>0$; for $E>0$ there is no growing solution. Thus, the question of the stability of the solution $\varphi_0(x)$ reduces to the problem of finding the minimum positive eigenvalue of Eq. (23). If all the eigenvalues are negative, then the solution is stable. (Notice that the stability of the solu-

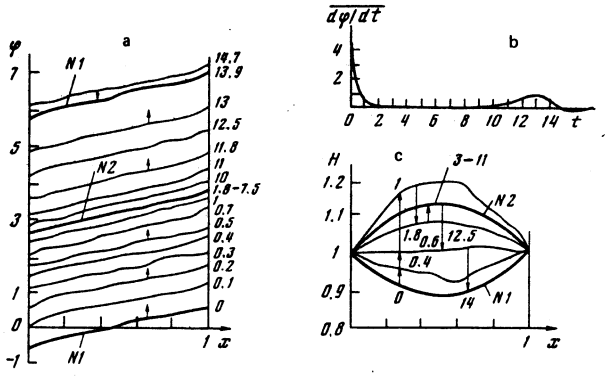

FIG. 13. Evolution of the stable solutions 1 ($L=1$, $H_e=1$, $\varphi(0)=-0.4628$) under the action of an initial impulse $\dot{\varphi}(x, t=0)=4.5361$: *a*) evolution of the phase φ; *b*) variation with time of the mean (with respect to the coordinate x) speed $\overline{d\varphi/dt}$ (i.e., of the voltage potential in the barrier); it can be seen that in the course of the evolution the solution is retarded in the vicinity of the unstable distribution 2 (in the time interval $2\lesssim t\lesssim 10$); *c*) the evolution of the field $H=d\varphi/dx$.

tion does not depend on the presence of the decrement β; on it depends only the magnitude of the increment (25). In the numerical computations carried out by us the parameter β was chosen to be equal to $\beta=1$.)

The general solution to Eq. (23) can be expressed in terms of the Lamé functions (cf. Ref. 5), but it is then difficult to effectively find the eigenvalues. Therefore, the eigenvalues were found numerically by a direct calculation of Eq. (23) with the aid of a WANG-2200 computer. The results obtained show that all the specific solutions of the anomalous type (see the Introduction) investigated by us are unstable. Only the solutions with the numbers $N=2n+1$ (see (6)), which correspond to the normal vortex structure (cf. Ref. 7), and which are depicted in Figs. 5–10 by the heavy curves, are stable.

The result, obtained on the basis of the (linearized) Eq. (23), that the anomalous solutions are unstable was verified directly by solving the partial differential equation (20) with the aid of a computer (cf. Ref. 11). It was found that, upon being sufficiently strongly perturbed, a stable solution goes over into another stable solution, but that in the process of evolution the solution assumes a form corresponding to an unstable state and can (in the case of a sufficiently small increment) retain the unstable form for a long time. (Examples of the evolution in time of the solutions are given in Figs. 12 and 13.) The latter implies that such solutions could, in principle, manifest themselves in experiment (for example, they could affect the value of the switching time between stable, stationary states in devices based on the use of the Josephson effects). The problems connected with stability analysis and the nonstationary solutions of Eq. (20) will be considered separately in greater detail.

In conclusion, let us note that Eq. (20) with $\beta=0$ coincides with the so-called sine-Gordon equation, which is widely discussed in the literature in connection with the search for quasiclassical solutions for elementary particles.[12] The same type of equation is used in, for example, the dynamical theory of dislocations.[13-15] In view of this, it seems that the description of the particular solutions of this equation and the analysis of their stability (to which the present paper is devoted) can also be of interest in other problems.

[1)] Notice that for the symmetric boundary conditions (3) the problem admits of both symmetric (for example, 1 and 2) and nonsymmetric (for example, 3 and 4) field distributions inside the barrier (see Figs. 1b and 2b). Here we have an example of the so-called broken symmetry.

[2)] The numerical calculations were carried out on a computer of the WANG-2200 type.

[1]R. A. Ferrell and R. E. Prange, Phys. Rev. Lett. **10**, 479 (1963).

[2]I. O. Kulik, Zh. Eksp. Teor. Fiz. **51**, 1952 (1966) [Sov. Phys. JETP **24**, 1307 (1967)].

[3]I. O. Kulik and I. I. Yanson, Éffekt Dzhozefsona v sverkhprovodyashchikh tunnel'nykh strukturakh (The Josephson Effect in Superconducting Tunneling Structures), Nauka, 1970 (Eng. Transl. Halsted Press, New York, 1972).

[4]C. S. Owen and D. J. Scalapino, Phys. Rev. **164**, 538 (1967).

[5]P. Lebwohl and M. J. Stephen, Phys. Rev. **163**, 376 (1967).

[6]L. Solymar, Superconductive Tunneling and Applications, Wiley-Interscience, New York, 1972 (Russ. Transl., Mir, 1974).

[7]G. F. Zharkov, Zh. Eksp. Teor. Fiz. **71**, 1951 (1976) [Sov. Phys. JETP **44**, 1023 (1976)].

[8]A. A. Andronov, A. A. Vitt, and S. É. Khaĭkin, Teoriya kolebaniĭ (The Theory of Oscillations), Fizmatgiz, 1959 (Eng. Transl., Pergamon, New York, 1966).

[9]V. L. Ginzburg, Usp. Fiz. Nauk **48**, 25 (1952).

[10]O. V. Lounasmaa, Experimental Principles and Methods below 1 K, Academic Press, New York, 1974.

[11]S. Hasuo, T. Imamura, and K. Dazai, Proc. Intern. Conf. on Superconducting Quantum Devices, West Berlin, October 5–8, 1976, p. 10.

[12]A. Neven, Phys. Rep. (ed. J. L. Gervais) **23C**, No. 2 (1976).

[13]J. Frenkel and T. Kontorova, Phys. Z. Sowjetunion **13**, 1 (1938).

[14]A. Seeger and A. Kochendorfer, Z. Phys. **130**, 321 (1951).

[15]A. Seeger, H. Dorth, and A. Kochendorfer, Z. Phys. **134**, 173 (1953).

Translated by A. K. Agyei